Tailoring multiple porosities of hierarchical ZSM-5 zeolites by carbon dots for high-performance catalytic transformation

*Shufang Zhao, Kyung Duk Kim, Lizhuo Wang, Ryong Ryoo, and Jun Huang**

Dr. S. Zhao, Dr. L. Wang, Prof. J. Huang
Laboratory for Catalysis Engineering, School of Chemical and Biomolecular Engineering, Sydney Nano Institute, The University of Sydney, NSW 2006, Australia
E-mail: jun.huang@sydney.edu.au

Dr. K. Kim, Prof. R. Ryoo
Center for Nanomaterials and Chemical Reactions, Institute for Basic Science (IBS), Daejeon 305-701, Korea

Prof. R. Ryoo
Department of Chemistry, KAIST, Daejeon 305-701, Korea

Keywords: hierarchical ZSM-5 zeolites, carbon dots, acidity, TIPB cracking, ethanol dehydration

A simple and high-efficiency method has been proposed to synthesize hierarchical ZSM-5 zeolites with micropore and multistage mesopores by adopting water-soluble carbon dots (CDots) with various size distributions, such as 1-stage size distribution of CDots-1 of around 23 nm, 2-stage size distribution of CDots-2 of 6 nm and 9 nm, 3-stage size distribution of CDots-3 of 5 nm, 8 nm, and 18 nm. The abundant –OH and –COOH groups on the surface of CDots provide the high solubility in water. The characterization techniques confirmed that the dual-porous h-ZSM-5 (MIcro–mEsopores, M-IE) and multi-porous h-ZSM-5 (MIcro–mEso–mEsopores, M-IEE), h-ZSM-5 (MIcro–mEso–mEso-mEsopores, M-IEEE) catalysts have been obtained. Notably, the hierarchical ZSM-5(M-IEEE) catalyst with micropore of 0.55 nm, two small mesopores of 4.8 nm, 7.4 nm, and one large mesopore of 17.5 nm showed excellent catalytic performance with the highest TIPB cracking conversion (97.3%) and high stability. Similarly, the h-ZSM-5(M-IEEE) showed the high ethanol to olefins (ETO) conversion (100%). The improved catalytic activity can be attributed to the more efficient diffusion of reactants and products in the crystals with the help of multistage mesopores, improved anti-coking stability, combined with the effect of suitable acidity and the increased accessibility of the acid sites.

1. Introduction

The ZSM-5 zeolites have played a vital role in the chemical industry for a series of reactions, such as methanol-to-hydrocarbons (MTH) process and the disproportionation to xylene, due to its ordered microporous structure (0.55 nm).[1-4] However, for many reactions involving bulky molecules, conventional ZSM-5 zeolites often suffer from diffusion effects that eventually lead to rapid deactivation.[5-11] Nowadays, preparing hierarchical ZSM-5 zeolites with micro- and meso- or macroporosity has aroused considerable attention.[12-17] The hierarchical ZSM-5 zeolites combine at least dual porosities (micro-mesopores and micro-macropores),[15] which could gain efficient mass transfer and thereby avoiding rapid deactivation. Kunhao Li et al.[11] indicated 1) the intracrystalline-diffusion mechanism that occurs in micropores of zeolites; 2) diffusion in mesopores mainly follows the Knudsen-diffusion mechanism; and 3) diffusion in macropores follows the molecular-diffusion mechanism. The activation energy of intracrystalline-diffusion in micropores is much higher than that in mesopores (Knudsen) or macropores (molecular).[9,11] Therefore, the hierarchical ZSM-5 zeolites with dual porosities exhibit positive effects on activity, selectivity, and stability due to their better transport properties and the accessibility to the active sites, in comparison with microporous ZSM-5 zeolites.[9,15] With respect to dual porosities of hierarchical ZSM-5 zeolites, multiple porosities of hierarchical ZSM-5 zeolites can be used to promote a combination of two and more sequential reactions with many synergistic effects.[15] The suitable channels and required acidity in micropores and small mesopores are equally important.[18] Therefore, the hierarchical ZSM-5 zeolites containing multiple porosities (micro-meso-mesopores and micro-meso-macropores) present the advantages associated with each level of porosity.[19]

A series of synthesis methods have been developed to synthesize the hierarchical ZSM-5 zeolites. The ZSM-5 zeolites with micro-mesoporous structures can generally be synthesized through hard templating methods[20-24] involving the utilization of solid materials (for example,

carbonaceous materials,[20] polymers,[25] aerogels,[26,27] as well as inorganic solid materials[28]), soft templating methods,[1,29] and post-treatments.[30-33] The ZSM-5 zeolites with micro-macroporous structures can be achieved by preparing hollow ZSM-5 with carbon black microspheres as templates.[14,19] The hierarchical zeolites with micro-meso-macroporous structures have been synthesized by a quasi-solid state crystallization process.[15,19,34] Baolian Su et al.[13] designed the hierarchical zeolites by Murray's law, indicating that the porosity distribution in the resultant zeolites followed Murray's law. However, so far, the construction of hierarchical ZSM-5 zeolites possessing multiple porosities (micro and multi-mesopores) remains a huge challenge.

Carbon is commonly a black material, which is considered to have low solubility in water. Carbon dots (CDots) are a new member of carbon nanomaterials with a lot of -COOH and -OH functional groups on their surface.[35-38] Thus, compared to traditional carbon nanomaterials, CDots are superior in terms of excellent water solubility as the template for hierarchical zeolite synthesis. In general, CDots could be synthesized by two routes, namely the top-down route and the bottom-up route.[38] In our work, we prepared three CDots with different size distributions simply by the top-down route, which breaking down larger carbon structures by laser ablation and electrochemical oxidation or chemical oxidation.[39,40] To the best of our knowledge, the application of water-soluble CDots in the synthesis of multiple porosities of hierarchical ZSM-5 zeolites has not yet been explored. Only a class composites of CDots in zeolites have been synthesized,[41] for example, CNDs@zeolite composites,[42] CNDs@MgAPO-44,[43] CNPs@MgAPO-44.[44] The micropores of the zeolite host lattice offer a favorable microscopic environment for the facile regulation and stabilization of the ultrafine CDots.

In the present work, we demonstrate the synthesis of ZSM-5 zeolites with dual and multiple pores through the use of water-soluble CDots with different sizes as templates, such as 1-stage size distribution of CDots-1 of around 23 nm, 2-stage size distribution of CDots-2 of

6 nm and 9 nm, 3-stage size distribution of CDots-3 of 5 nm, 8 nm, and 18 nm. It is expected that these hierarchical ZSM-5 zeolites will provide a basis for studying the mass-transfer limitation on the catalytic performance of zeolite catalysts. The catalytic cracking of big molecular size 1,3,5-triisopropylbenzene (TIPB) and the catalytic dehydration of small molecular size ethanol were selected as testing reactions in our work. The effect of different levels of porosity in hierarchical ZSM-5 zeolites on these reactions will be investigated.

2. Results and Discussion

2.1. Physicochemical Properties of the CDots Samples and As-synthesized ZSM-5 Zeolites

We prepared CDots samples according to the Experiment Section. The particle size distributions of CDots samples measured by dynamic light scattering (DLS) are shown in **Figure 1**a. The 1-stage size distribution of CDots-1 is around 23 nm, the 2-stage size distribution of CDots-2 is centered at 6 nm and 9 nm, and CDots-3 presents 3-stage size distribution of 5 nm, 8 nm, and 18 nm. **Figure 1**b shows the wide-angle XRD patterns of the as-synthesized microporous and hierarchical ZSM-5 zeolites by CDots' templates. From **Figure 1**b, the typical MFI structure of as-prepared microporous m-ZSM-5, hierarchical h-ZSM-5 (MIcro–mEsopores, M-IE) prepared by CDots-1 template, h-ZSM-5 (MIcro–mEso–mEsopores, M-IEE) prepared by CDots-2 template, and h-ZSM-5 (MIcro–mEso–mEso-mEsopores, M-IEEE) prepared by CDots-3 template have been confirmed due to the observation of diffraction peaks at 2θ equal to 7.9°, 8.8°, 23.1°, and 23.8°.[14,45,46] Moreover, in the small angle XRD region, as can be seen from **Figure S1**, a well-defined peak at 2θ of 1.25° to 2.1° could be observed in all hierarchical ZSM-5 zeolites, demonstrating their highly order hexagonal mesostructured matrix.[14]

As shown in **Figure 1**c, the dual-porosity and multi-porosity of the as-synthesized hierarchical ZSM-5 zeolites were demonstrated by the N_2 adsorption-desorption isotherms measured with a Quantachrome Autosorb IQ-C at 77 K. The m-ZSM-5 presents the typical

type-I profile of microporous zeolites. Differently, the h-ZSM-5(M-IE), h-ZSM-5(M-IEE) and h-ZSM-5(M-IEEE) zeolites show the obvious hysteresis loops of type H4, exhibiting a distinct feature of hierarchical zeolites containing both micropores and mesopores.[47] The corresponding pore properties are summarized in **Table 1**. Compared to the m-ZSM-5 (S_{BET} = 323 m^2 g^{-1}, V_{total} = 0.22 cm^3 g^{-1}), all the h-ZSM-5 zeolites possessing dual-pore or multi-pore reveal a larger total surface area (S_{BET} = 410-432 m^2 g^{-1}) and total pore volume (V_{total} = 0.44-0.52 cm^3 g^{-1}). There is no significant change in mesopore surface area (S_{meso}) and mesopore volume (V_{meso}) for all the h-ZSM-5 zeolites.

Pore size distributions for the as-synthesized dual-porosity and multi-porosity of hierarchical ZSM-5 zeolites calculated by the Barrett–Joyner–Halenda (BJH) method from the adsorption branch are presented in **Figure 1**d. Regardless of micropores, the hierarchical h-ZSM-5(M-IE) zeolite reflects a pore size distribution with mesopores of about 21.8 nm (**Figure 1**d). The h-ZSM-5(M-IEE) zeolite exhibits a pore size distribution with two-stage mesopores centered at 5.5 nm and 8.5 nm, respectively (**Figure 1**d). The h-ZSM-5(M-IEEE) zeolite presents a three-stage mesopore distribution (4.8 nm, 7.4 nm, and 17.5 nm) (**Figure 1**d). They are similar to the size distribution of CDots.

The TEM images in **Figure 1**e and **1**f reveal that h-ZSM-5(M-IEE) and h-ZSM-5(M-IEEE) zeolites are formed with multiple porosities. Combined with the above results, the dual-porosity (h-ZSM-5(M-IE)) and multi-porosity (h-ZSM-5(M-IEE) and h-ZSM-5(M-IEEE)) of hierarchical ZSM-5 with the comparable mesoporous surface area (S_{meso} = 245-260 m^2 g^{-1}) and V_{meso} (0.30 to 0.36 cm^3 g^{-1}) but different levels of porosity have been obtained by using CDots as templates.

2.2. Acid Properties of the As-synthesized ZSM-5 Catalyst Materials

In order to gain the local structure of Al species in the as-synthesized dual-porosity and multi-porosity of hierarchical ZSM-5 zeolites, ^{27}Al MAS NMR experiments were conducted to confirm the coordination state of Al in the zeolites (**Figure 2**a). A strong peak at around 54 ppm

assigned to tetra-coordinated framework aluminum (Al^{IV}) species was observed in all ZSM-5 zeolites.[48-50] Moreover, compared with the tetrahedral Al signal, the weak peak at around 0 ppm is assigned to octahedral coordinated aluminum (Al^{VI}) species, which is from extraframework Al.[48-50] It is worth noting that the framework Al^{IV} species contributing to the Brønsted acid site (SiOHAl) in ZSM-5 zeolites. Thus, our ^{27}Al MAS NMR results indicate that most of the Al atoms are inserted in the framework of hierarchical ZSM-5 zeolite as Al^{IV} species, thereby forming Brønsted acid site.

The ^{31}P-TMPO NMR is an effective method to characterize the acid properties of ZSM-5 zeolites.[51-53] **Figure 2**b-d shows the ^{31}P MAS NMR spectra of TMPO adsorbed on the as-synthesized dual-porosity and multi-porosity of hierarchical ZSM-5 zeolites. In all ZSM-5 zeolites under study, five distinct ^{31}P resonance peaks at 84, 76, 68, 64, and 62 ppm were observed, which can be assigned to the $TMPOH^+$ adsorbed on the different Brønsted acid sites with varied acid strengths (denoted as I, II, III, IV, and V), respectively.[51,52,54] The highest δ_{31P} value (84 ppm) reflects the Brønsted acid sites with the highest acid strengths in the hierarchical ZSM-5 zeolites.[53,54] In addition, the peaks at 42-52 and 30 ppm can be assigned to the weakly physisorbed and mobile TMPO, respectively.[51,52]

Furthermore, according to the calculation method of acid concentration in the literature,[51,53] the acid concentration of the five Brønsted acid sites (I, II, III, IV, and V) was summarized in **Table 2**. The total acid concentration (A_{tot}) in **Table 2** indicates that the dual-porous h-ZSM-5(M-IE) and multi-porous h-ZSM-5(M-IEE) possess the nearly same total concentration of Brønsted acid sites and slightly more than the total Brønsted acid concentration of the multi-porous h-ZSM-5(M-IEEE) zeolites. Obviously, h-ZSM-5(M-IEEE) has a higher concentration of strong Brønsted acid sites (I (84) + I (76) = 212 × 10^{-5} mol g^{-1}) than h-ZSM-5(M-IE) (I (84) + I (76) = 161 × 10^{-5} mol g^{-1}) and h-ZSM-5(M-IEE) (I (84) + I (76) = 169 × 10^{-5} mol g^{-1}) zeolites. The actual Si/Al_2 ratios for four ZSM-5 zeolites obtained by the ICP test are 46.0 for m-ZSM-5, 47.2 for h-ZSM-5(M-IE), 47.0 for h-ZSM-5(M-IEE), and 46.8 for h-

ZSM-5(M-IEEE), respectively (**Table 1**). Clearly, the input Si/Al_2 ratios (around 50) and actual Si/Al_2 ratios for four ZSM-5 zeolites are all similar. It can indicate that all the ZSM-5 zeolites have a comparable content of acid sites. To further evaluate the acidity of the as-synthesized hierarchically porous ZSM-5 zeolites, NH_3-TPD profiles have been illustrated in **Figure S2**. Two distinct peaks can be observed, which are attributed to the release of NH_3 from a weak Brønsted acid sites and stronger Brønsted acid sites, respectively. Meanwhile, the quantitative results from NH_3-TPD profiles have been summarized in **Table 2**. These results are consistent with their ^{31}P NMR analysis of absorbed TMPO.

2.3. Catalytic Performances of As-synthesized ZSM-5 Catalyst Materials

In order to verify the advantage of the multiple porosities of hierarchical ZSM-5 zeolites, the cracking of 1, 3, 5-triisopropylbenzene (TIPB) was carried out at 500 °C under atmospheric pressure in a vertical fixed-bed quartz reactor. It is well known that TIPB molecular with a dynamic diameter of 0.94 nm is significantly larger than the micropores of m-ZSM-5 with a dynamic diameter of 0.56 nm, the cracking of TIPB is considered to occur only on the external surface of microporous ZSM-5 zeolites.[6,8,55] The cracking of TIPB is thus a typical probe reaction for evaluating the catalytic performance of hierarchical zeolites.[6,55-58] Compared to the m-ZSM-5 catalyst, the dual-porous h-ZSM-5(M-IE) and multi-porous h-ZSM-5(M-IEE), h-ZSM-5(M-IEEE) catalysts synthesized by water-soluble CDots as templates provided significantly higher TIPB conversions. As shown in **Figure 3**a, in the initial reaction stages, the m-ZSM-5 gives a low TIPB conversion of 59% at 500 °C. And the TIPB conversion of different hierarchical ZSM-5 catalysts is over 90%, which decreases in the order of h-ZSM-5(M-IEEE) > h-ZSM-5(M-IE) > h-ZSM-5(M-IEE) > m-ZSM-5. The h-ZSM-5(M-IEEE) catalyst with three-stage mesoporous channels (4.8 nm, 7.4 nm, and 17.5 nm) has the highest TIPB cracking performance, although it possesses relatively lower concentration of total Brønsted acid sites (**Table 2**, $A_{tot} = 359 \times 10^{-5}$ mol g^{-1}).

Generally, diisopropylbenzene (DIPB), isopropylbenzene (IPB), and benzene (B) are the main products in the TIPB cracking (**Figure S3**). As shown in **Figure 3**b, compared with m-ZSM-5, the selectivities of IPB and B significantly increase over the hierarchical ZSM-5 catalysts, with decreasing the selectivity of DIPB, indicating that the increased accessibility of the acid sites resulting from the mesoporous structure favors to the cracking of TIPB and further cracking of DIPB. Also, the h-ZSM-5(M-IEEE) is believed to be a better catalyst for deep cracking.

The spent catalysts after the TIPB cracking reaction of 10 h at 500 °C were measured by Thermogravimetric analysis (TGA) in the air to investigate the carbonaceous residues. As shown in **Figure S4**a, the sequences of ZSM-5 catalysts in total amount of carbonaceous species are m-ZSM-5 (8.6%) > h-ZSM-5(M-IE) (5.3%) > h-ZSM-5(M-IEE) (4.1%) > h-ZSM-5(M-IEEE) (2.9%). More specifically, sample h-ZSM-5(M-IEEE) with micropore of 0.55 nm, two small mesopores of 4.8 nm, 7.4 nm, and one large mesopore of 17.5 nm decrease the coke formation and enable carbonaceous compounds to move out of the pore quickly, thus leading to a prolonged lifetime of h-ZSM-5(M-IEEE) catalyst. Furthermore, UV-Vis spectroscopy was performed to examine the carbonaceous species on the surfaces of the catalysts after the cracking reaction of TIPB (**Figure S4**b). The intensities of the peaks in the region of 200-300 nm assigned to the formation of low-polycyclic hydrocarbons on the surface of the hierarchical ZSM-5 catalysts display an obvious increase compared with that of the m-ZSM-5 catalyst. The possible reason is the increase of the mesopore surface area (S_{meso}) and mesopore volume (V_{meso}) of the hierarchical ZSM-5 catalysts. And the absorption peaks around 660 nm are likely due to the formation of large poly-aromatic compounds on the surface of the catalysts.[59] As observed in **Figure S4**b, for the hierarchical ZSM-5 catalysts, there has been a considerable decrease in the formation amount of the large poly-aromatic compounds compared with m-ZSM-5 catalyst. Especially, for the spent h-ZSM-5(M-IEEE) catalyst, few poly-aromatic compounds were detected. Also, we confirm that, after regenerating the spent h-ZSM-5(M-IEEE) in the air at

570 °C for 10 h, the reactivated h-ZSM-5(M-IEEE)-Re displays high TIPB cracking conversion, stability and selectivity of deep cracking products similar to the fresh h-ZSM-5(M-IEEE) (**Figure S5**).

Pore condensation according to the Kelvin equation may explain the higher TIPB cracking activity and the lower deactivation rate on the h-ZSM-5(M-IE) than on h-ZSM-5(M-IEE).[60,61] The Kelvin equation indicates that the smaller mesopore size results in the more pronounced pore condensation.[60,61] The multi-porous h-ZSM-5(M-IEE) with micropore of 0.55 nm and two-stage small mesopores of 5.5 nm and 8.5 nm may suffer more significant pore condensation, and thus causes relative lower activity and shorter lifetime than dual-porous h-ZSM-5(M-IE) with one-stage large mesopores of 21.8 nm. Most importantly, multi-porous h-ZSM-5(M-IEEE) with micropore of 0.55 nm, two small mesopores of 4.8 nm, 7.4 nm, and one large mesopore of 17.5 nm has been confirmed the superiority in terms of TIPB cracking.

Similarly, the gas-phase dehydration reaction of ethanol was also carried out at 500 °C in a vertical fixed-bed quartz reactor.[62-67] It is generally accepted that the intramolecular dehydration of ethanol to ethene can occur as the main reaction at high temperature (500 °C under study).[68] The formation of bulky aromatic species that may lead to catalyst deactivation is due to further transformation of cyclic and light olefins.[69,70] A plausible reaction and deactivation network for ethanol conversion was depicted (**Figure S6**). As shown in **Figure 3**c, for all the catalysts, the ethanol is completely transformed at the initial stage. It is apparent that ethanol dehydration can occur on the Brønsted acid sites in the confinement environment of micropores.[66] The selectivity for main product ethene increases in the order of h-ZSM-5(M-IEEE) > h-ZSM-5(M-IE) > h-ZSM-5(M-IEE) > m-ZSM-5 (**Figure 3**d). The improved ethene selectivity may be related to reduced competition for the by-products or cokes. Additionally, as you can see from the **Figure 3**c, compared with the m-ZSM-5 catalyst, the dual-porous h-ZSM-5(M-IE) and multi-porous h-ZSM-5(M-IEE), h-ZSM-5(M-IEEE) catalysts greatly increase the

stability of ethanol dehydration reaction. Clearly, the stability of ethanol dehydration follows the order of h-ZSM-5(M-IEEE) > h-ZSM-5(M-IE) > h-ZSM-5(M-IEE) > m-ZSM-5. Remarkably, the hierarchical h-ZSM-5(M-IEEE) catalyst with micropore of 0.55 nm, two small mesopores of 4.8 nm, 7.4 nm, and one large mesopore of 17.5 nm is able to maintain a 100% ethanol conversion for longer than 30 h. Notably, the lowest amount of carbonaceous residues in spent h-ZSM-5(M-IEEE) catalyst (2.7%) could be observed (**Table S1**). The regenerated h-ZSM-5(M-IEEE)-Re catalyst obtains a similar good catalytic performance as that of the fresh h-ZSM-5(M-IEEE) towards ethanol conversion and ethene selectivity (**Figure S7**). The excellent catalytic performances of multi-porous h-ZSM-5(M-IEEE) catalyst in both testing reactions can be attributed to the multistage mesopores on the improvement of diffusion of reactants and products, coking resistance, stability, combined with the increased accessibility of the acid sites. Each level of porosity presents the advantages associated with selectivity to mass transport.

3. Conclusion

We demonstrate that water-soluble carbon dots can act as high-performance templates capable of producing high efficiency hierarchical ZSM-5 zeolites with micropore and multistage mesopores. 1-stage size distribution of CDots-1 of around 23 nm, 2-stage size distribution of CDots-2 of 6 nm and 9 nm, 3-stage size distribution of CDots-3 of 5 nm, 8 nm and 18 nm were adopted in our work. The characterization techniques confirmed that the obtained hierarchical ZSM-5 zeolites consisted of different levels of porosity (micro and multi-mesopores).

The dual-porous h-ZSM-5(M-IE) and multi-porous h-ZSM-5(M-IEE), h-ZSM-5(M-IEEE) catalysts exhibited higher conversion and enhanced coke resistance toward deactivation in the cracking of 1,3,5-trimethylbenzene and the dehydration of ethanol, as compared with conventional microporous ZSM-5 zeolites. The improved catalytic activity can be attributed to the more efficient diffusion of reactants and products in the crystals with the help of multistage

mesopores, improved coking resistance, and stability, combined with the increased accessibility of the acid sites. In particular, the h-ZSM-5(M-IEEE) catalyst with micropore of 0.55 nm, two small mesopores of 4.8 nm, 7.4 nm, and one large mesopore of 17.5 nm can offer the best catalytic performance.

Acknowledgements

This work was supported by the Australian Research Council Discovery Projects (DP150103842, DP180104010), the SOAR Fellowship, and the Sydney Nano Grand Challenge from the University of Sydney.

Received: ((will be filled in by the editorial staff))
Revised: ((will be filled in by the editorial staff))
Published online: ((will be filled in by the editorial staff))

References

[1] M. Choi, K. Na, J. Kim, Y. Sakamoto, O. Terasaki, R. Ryoo, *Nature* **2009**, *461*, 246.
[2] C. Wang, Q. Wang, J. Xu, G. Qi, P. Gao, W. Wang, Y. Zou, N. Feng, X. Liu, F. Deng, *Angew. Chem. Int. Ed.* **2016**, *55*, 2507.
[3] J. Zhang, L. Wang, B. Zhang, H. Zhao, U. Kolb, Y. Zhu, L. Liu, Y. Han, G. Wang, C. Wang, *Nat. Catal.* **2018**, *1*, 540.
[4] C. Wang, L. Wang, J. Zhang, H. Wang, J. P. Lewis, F.-S. Xiao, *J. Am. Chem. Soc.* **2016**, *138*, 7880.
[5] A. Corma, *J. Catal.* **2003**, *216*, 298.
[6] Y. Yan, X. Guo, Y. Zhang, Y. Tang, *Catal. Sci. Technol.* **2015**, *5*, 772.
[7] A. Ishihara, *Fuel Process. Technol.* **2019**, *194*, 106.
[8] M. Pan, J. Zheng, Y. Liu, W. Ning, H. Tian, R. Li, *J. Catal.* **2019**, *369*, 72.
[9] M. Hartmann, A. G. Machoke, W. Schwieger, *Chem. Soc. Rev.* **2016**, *45*, 3313.
[10] L. Meng, X. Zhu, W. Wannapakdee, R. Pestman, M. G. Goesten, L. Gao, A. J. van Hoof, E. J. Hensen, *J. Catal.* **2018**, *361*, 135.
[11] K. Li, J. Valla, J. Garcia‐Martinez, *ChemCatChem* **2014**, *6*, 46.
[12] A. Clauset, C. Moore, M. E. Newman, *Nature* **2008**, *453*, 98.
[13] Z. Peng, L.-H. Chen, M.-H. Sun, H. Zhao, Z. Wang, Y. Li, L.-Y. Li, J. Zhou, Z.-C. Liu, B.-L. Su, *Inorg. Chem. Front.* **2018**, *5*, 2829.
[14] X. Shen, W. Mao, Y. Ma, D. Xu, P. Wu, O. Terasaki, L. Han, S. Che, *Angew. Chem. Int. Ed.* **2018**, *57*, 724.
[15] X.-Y. Yang, L.-H. Chen, Y. Li, J. C. Rooke, C. Sanchez, B.-L. Su, *Chem. Soc. Rev.* **2017**, *46*, 481.
[16] M. Hartmann, W. Schwieger, *Chem. Soc. Rev.* **2016**, *45*, 3311.
[17] Y. Wei, T. E. Parmentier, K. P. de Jong, J. Zečević, *Chem. Soc. Rev.* **2015**, *44*, 7234.
[18] X. Y. Yang, G. Tian, L. H. Chen, Y. Li, J. C. Rooke, Y. X. Wei, Z. M. Liu, Z. Deng, G. Van Tendeloo, B. L. Su, *Chem. Eur. J.* **2011**, *17*, 14987.

[19] L.-H. Chen, X.-Y. Li, J. C. Rooke, Y.-H. Zhang, X.-Y. Yang, Y. Tang, F.-S. Xiao, B.-L. Su, *J. Mater. Chem.* **2012**, *22*, 17381.
[20] C. J. Jacobsen, C. Madsen, J. Houzvicka, I. Schmidt, A. Carlsson, *J. Am. Chem. Soc.* **2000**, *122*, 7116.
[21] V. Valtchev, B. J. Schoeman, J. Hedlund, S. Mintova, J. Sterte, *Zeolites* **1996**, *17*, 408.
[22] I. Schmidt, A. Boisen, E. Gustavsson, K. Ståhl, S. Pehrson, S. Dahl, A. Carlsson, C. J. Jacobsen, *Chem. Mater.* **2001**, *13*, 4416.
[23] C. Xue, T. Xu, J. Zheng, J. Wang, Z. Zhang, X. Hao, A. Abudula, G. Guan, *Mater. Lett.* **2015**, *154*, 55.
[24] S.-S. Kim, J. Shah, T. J. Pinnavaia, *Chem. Mater.* **2003**, *15*, 1664.
[25] B. T. Holland, L. Abrams, A. Stein, *J. Am. Chem. Soc.* **1999**, *121*, 4308.
[26] Y. Tao, Y. Hattori, A. Matumoto, H. Kanoh, K. Kaneko, *J. Phys. Chem. B* **2005**, *109*, 194.
[27] Y. Tao, H. Kanoh, K. Kaneko, *J. Am. Chem. Soc.* **2003**, *125*, 6044.
[28] A. G. Machoke, A. M. Beltrán, A. Inayat, B. Winter, T. Weissenberger, N. Kruse, R. Güttel, E. Spiecker, W. Schwieger, *Adv. Mater.* **2015**, *27*, 1066.
[29] M. Choi, H. S. Cho, R. Srivastava, C. Venkatesan, D.-H. Choi, R. Ryoo, *Nat. Mater.* **2006**, *5*, 718.
[30] V. Valtchev, G. Majano, S. Mintova, J. Pérez-Ramírez, *Chem. Soc. Rev.* **2013**, *42*, 263.
[31] S. Yang, C. Yu, L. Yu, S. Miao, M. Zou, C. Jin, D. Zhang, L. Xu, S. Huang, *Angew. Chem. Int. Ed.* **2017**, *56*, 12553.
[32] J. Wang, Z. Zhong, K. Ding, B. Zhang, A. Deng, M. Min, P. Chen, R. Ruan, *Energy Convers. Manage.* **2017**, *147*, 100.
[33] R. Feng, X. Yan, X. Hu, Y. Wang, Z. Li, K. Hou, J. Lin, *J. Porous Mater.* **2018**, *25*, 1.
[34] L. H. Chen, X. Y. Li, G. Tian, Y. Li, H. Y. Tan, G. Van Tendeloo, G. S. Zhu, S. L. Qiu, X. Y. Yang, B. L. Su, *ChemSusChem* **2011**, *4*, 1452.
[35] H. Li, R. Liu, W. Kong, J. Liu, Y. Liu, L. Zhou, X. Zhang, S.-T. Lee, Z. Kang, *Nanoscale* **2014**, *6*, 867.
[36] H. Li, Z. Kang, Y. Liu, S.-T. Lee, *J. Mater. Chem.* **2012**, *22*, 24230.
[37] H. Li, X. He, Z. Kang, H. Huang, Y. Liu, J. Liu, S. Lian, C. H. A. Tsang, X. Yang, S. T. Lee, *Angew. Chem. Int. Ed.* **2010**, *49*, 4430.
[38] S. Y. Lim, W. Shen, Z. Gao, *Chem. Soc. Rev.* **2015**, *44*, 362.
[39] J. M. Bai, L. Zhang, R. P. Liang, J. D. Qiu, *Chem. Eur. J.* **2013**, *19*, 3822.
[40] J. Shen, Y. Zhu, X. Yang, C. Li, *Chem. Commun.* **2012**, *48*, 3686.
[41] J. Liu, N. Wang, Y. Yu, Y. Yan, H. Zhang, J. Li, J. Yu, *Sci. Adv.* **2017**, *3*, e1603171.
[42] Y. Mu, H. Shi, Y. Wang, H. Ding, J. Li, *J. Mater. Chem. C* **2017**, *5*, 10894.
[43] Y. Mu, N. Wang, Z. Sun, J. Wang, J. Li, J. Yu, *Chem. Sci.* **2016**, *7*, 3564.
[44] Y. Xiu, Q. Gao, G.-D. Li, K.-X. Wang, J.-S. Chen, *Inorg. Chem.* **2010**, *49*, 5859.
[45] C. Lago, H. Decolatti, L. G. Tonutti, B. Dalla Costa, C. Querini, *J. Catal.* **2018**, *366*, 16.
[46] S. Lai, D. Meng, W. Zhan, Y. Guo, Y. Guo, Z. Zhang, G. Lu, *RSC Adv.* **2015**, *5*, 90235.
[47] M. Thommes, *Chem. Ing. Tech.* **2010**, *82*, 1059.
[48] S. Sklenak, J. Dědeček, C. Li, B. Wichterlova, V. Gabova, M. Sierka, J. Sauer, *Phys. Chem. Chem. Phys.* **2009**, *11*, 1237.
[49] P. Sazama, B. Wichterlova, J. Dedecek, Z. Tvaruzkova, Z. Musilova, L. Palumbo, S. Sklenak, O. Gonsiorova, *Microporous Mesoporous Mater.* **2011**, *143*, 87.
[50] C. Li, A. Vidal-Moya, P. J. Miguel, J. Dedecek, M. Boronat, A. Corma, *ACS Catal.* **2018**, *8*, 7688.
[51] Y. Seo, K. Cho, Y. Jung, R. Ryoo, *ACS Catal.* **2013**, *3*, 713.

[52] A. Zheng, S.-J. Huang, S.-B. Liu, F. Deng, *Phys. Chem. Chem. Phys.* **2011**, *13*, 14889.
[53] Q. Zhao, W.-H. Chen, S.-J. Huang, Y.-C. Wu, H.-K. Lee, S.-B. Liu, *J. Phys. Chem. B* **2002**, *106*, 4462.
[54] A. Zheng, S.-J. Huang, W.-H. Chen, P.-H. Wu, H. Zhang, H.-K. Lee, L.-C. De Menorval, F. Deng, S.-B. Liu, *J. Phys. Chem. A* **2008**, *112*, 7349.
[55] K. A. Tarach, K. Góra-Marek, J. Martinez-Triguero, I. Melián-Cabrera, *Catal. Sci. Technol.* **2017**, *7*, 858.
[56] X. H. Vu, T. T. Truong, U. Armbruster, A. Martin, *React. Kinet. Mech. Cat.* **2018**, *124*, 437.
[57] X. H. Vu, T. T. Truong, U. Armbruster, *J. Porous Mater.* **2018**, 1.
[58] P. Morales-Pacheco, J. Domínguez, L. Bucio, F. Alvarez, U. Sedran, M. Falco, *Catal. Today* **2011**, *166*, 25.
[59] S. P. Verkleij, G. T. Whiting, D. Pieper, S. P. Esclapez, S. Li, M. M. Mertens, M. Janssen, A. J. Bons, M. Burgers, B. M. Weckhuysen, *ChemCatChem* **2019**, *11*, 4788.
[60] H. Zhang, Z. Hu, L. Huang, H. Zhang, K. Song, L. Wang, Z. Shi, J. Ma, Y. Zhuang, W. Shen, *ACS Catal.* **2015**, *5*, 2548.
[61] C. Hulteberg, A. Leveau, J. G. M. Brandin, *Top. Catal.* **2013**, *56*, 813.
[62] T. K. Phung, L. P. Hernández, A. Lagazzo, G. Busca, *Appl. Catal. A* **2015**, *493*, 77.
[63] Q. Sheng, S. Guo, K. Ling, L. Zhao, *J. Braz. Chem. Soc.* **2014**, *25*, 1365.
[64] D. Fan, D.-J. Dai, H.-S. Wu, *Materials* **2013**, *6*, 101.
[65] L. Emdadi, Y. Wu, G. Zhu, C.-C. Chang, W. Fan, T. Pham, R. F. Lobo, D. Liu, *Chem. Mater.* **2014**, *26*, 1345.
[66] D. Liu, A. Bhan, M. Tsapatsis, S. Al Hashimi, *ACS Catal.* **2010**, *1*, 7.
[67] Q. Sheng, K. Ling, Z. Li, L. Zhao, *Fuel Process. Technol.* **2013**, *110*, 73.
[68] X. Zhang, R. Wang, X. Yang, F. Zhang, *Microporous Mesoporous Mater.* **2008**, *116*, 210.
[69] N. Viswanadham, S. K. Saxena, J. Kumar, P. Sreenivasulu, D. Nandan, *Fuel* **2012**, *95*, 298.
[70] U. V. Mentzel, S. Shunmugavel, S. L. Hruby, C. H. Christensen, M. S. Holm, *J. Am. Chem. Soc.* **2009**, *131*, 17009.

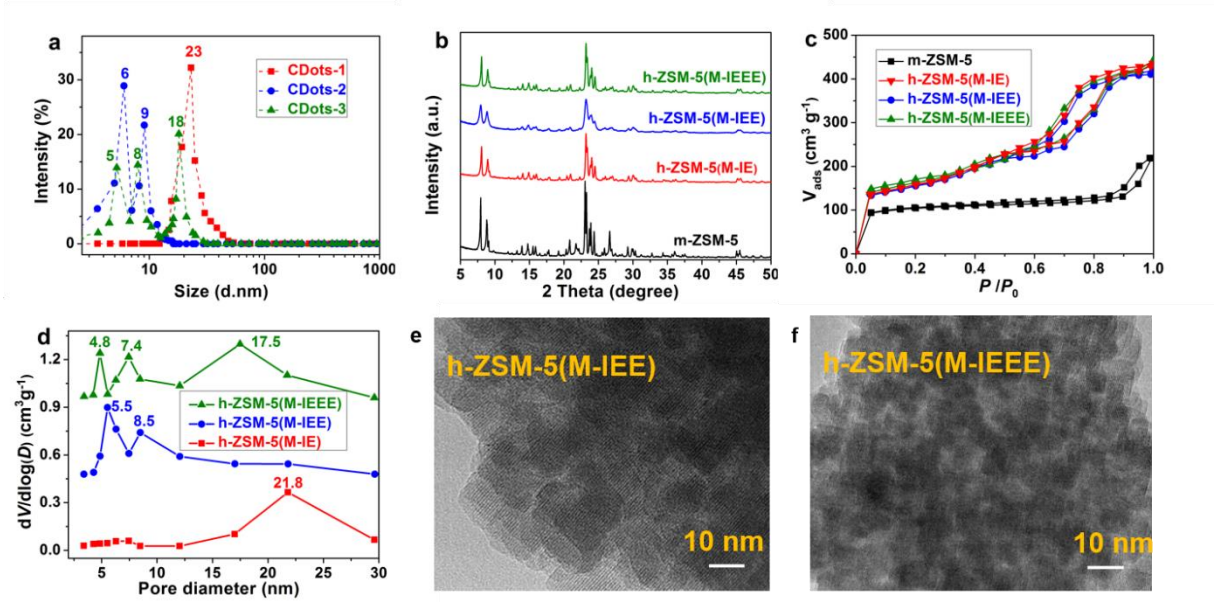

Figure 1. (a) Particle size distributions of CDots samples determined by dynamic light scattering (DLS), (b) Wide-angle XRD patterns for the as-synthesized microporous and hierarchically porous ZSM-5 zeolites, (c) Nitrogen adsorption-desorption isotherms of the as-synthesized microporous and hierarchically porous ZSM-5 zeolites, (d) BJH pore size distribution of the as-synthesized hierarchically porous ZSM-5 zeolites, (e) TEM images of the as-synthesized hierarchical h-ZSM-5(M-IEE) zeolite, and (f) TEM images of the as-synthesized hierarchical h-ZSM-5(M-IEEE) zeolite.

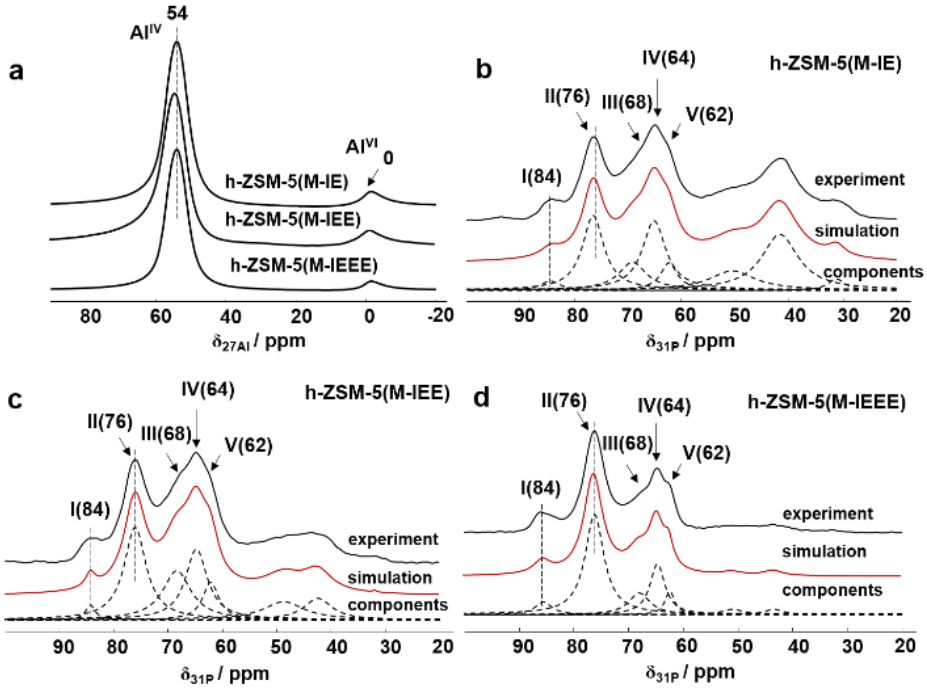

Figure 2. Solid-state NMR characterization of as-synthesized ZSM-5 zeolites. (a) ^{27}Al MAS NMR spectra of the as-synthesized hierarchically porous ZSM-5 zeolites, (b) ^{31}P MAS NMR spectrum of TMPO adsorbed on hierarchical h-ZSM-5(M-IE), (c) ^{31}P MAS NMR spectrum of TMPO adsorbed on hierarchical h-ZSM-5(M-IEE), and (d) ^{31}P MAS NMR spectrum of TMPO adsorbed on hierarchical h-ZSM-5(M-IEEE).

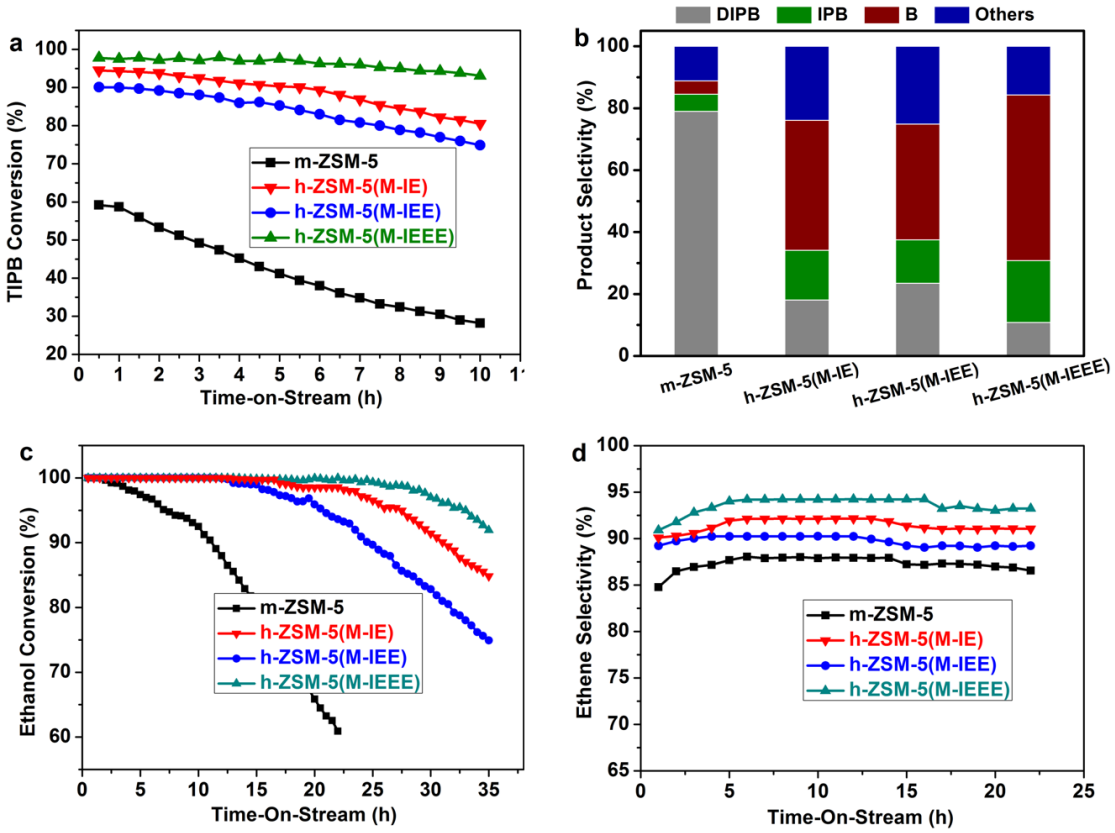

Figure 3. Catalytic performances of as-synthesized microporous and hierarchically porous ZSM-5 catalysts. (a) Effect of time on stream on conversion of 1, 3, 5-triisopropylbenzene (TIPB) cracking, (b) Product selectivity at TOS of 1 h in the TIPB cracking, (c) Effect of time on stream on ethanol conversion, and (d) Effect of time on stream on ethene selectivity in the ethanol dehydration. The carbon balance in all runs was over 90%.

Table 1. Si/Al_2 ratios[a)] and pore properties[b)] of as-synthesized microporous and hierarchically porous ZSM-5 zeolites.

zeolites	Si/Al_2	S_{BET} ($m^2\ g^{-1}$)	S_{meso} ($m^2\ g^{-1}$)	V_{total} ($cm^3\ g^{-1}$)	V_{meso} ($cm^3\ g^{-1}$)
m-ZSM-5	46.0	323	88	0.22	0.14
h-ZSM-5(M-IE)	47.2	432	260	0.52	0.36
h-ZSM-5(M-IEE)	47.0	410	245	0.44	0.30
h-ZSM-5(M-IEEE)	46.8	429	258	0.49	0.34

[a)] The Si/Al_2 ratio was determined by inductively coupled plasma optical emission spectroscopy (ICP-OES); [b)] BET specific surface area (S_{BET}) determined by Brunauer-Emmett-Teller (BET) method. Total pore volume (V_{total}) calculated by absorbed volume at $p/p_0 = 0.95$. Mesopore volume (V_{meso}) obtained by the t-plot method.

Table 2. The concentration of Brønsted acid sites calculated by ^{31}P MAS NMR of adsorbed TMPO and NH_3-TPD results.

zeolites	Brønsted acid sites titrated by TMPO ($\times 10^{-5}$ mol g^{-1})					A_{tot}[b)] ($\times 10^{-5}$ mol g^{-1})	$A_{tot\text{-}NH3}$[c)] ($\times 10^{-5}$ mol g^{-1})
	I(84)[a)]	II(76)	III(68)	IV(64)	V(62)		
h-ZSM-5(M-IE)	16.3	144.7	70.5	147.9	41.1	420	546
h-ZSM-5(M-IEE)	11.1	157.8	107.6	120.4	47.6	444	571
h-ZSM-5(M-IEEE)	21.5	190.5	47.1	77.1	22.7	359	470

[a)] The value indicates the chemical shift (δ_{31P}) of adsorbed TMPO; [b)] The total acid concentration obtained by ^{31}P MAS NMR of adsorbed TMPO; [c)] The total acid concentration determined by NH_3-TPD.

It is the first time to report that hierarchical ZSM-5 zeolites with micropore and multistage mesopores by adopting water-soluble carbon dots with different size distributions as templates. The hierarchical h-ZSM-5(M-IEEE) catalyst with micropore of 0.55 nm and multistage mesopores of 4.8, 7.4, and 17.5 nm showed excellent catalytic performance in TIPB cracking and ethanol to olefins (ETO).

S. Zhao, K. Kim, L. Wang, R. Ryoo, and J. Huang*

Tailoring multiple porosities of hierarchical ZSM-5 zeolites by carbon dots for high-performance catalytic transformation